



MOX–Report No. 27/2011

A Mimetic Discretization of Elliptic Control Problems

ANTONIETTI, P.F.; BIGONI, N.; VERANI, M.

MOX, Dipartimento di Matematica “F. Brioschi”
Politecnico di Milano, Via Bonardi 9 - 20133 Milano (Italy)

mox@mate.polimi.it

<http://mox.polimi.it>

A Mimetic Discretization of Elliptic Control Problems

Paola F. Antonietti

MOX, Dipartimento di Matematica, Politecnico di Milano,
Piazza Leonardo da Vinci 32, I-20133 Milano, Italy

E-mail: paola.antonietti@polimi.it

Nadia Bigoni

MOX, Dipartimento di Matematica, Politecnico di Milano,
Piazza Leonardo da Vinci 32, I-20133 Milano, Italy

E-mail: nadia.bigoni@mail.polimi.it

Marco Verani

MOX, Dipartimento di Matematica, Politecnico di Milano,
Piazza Leonardo da Vinci 32, I-20133 Milano, Italy

E-mail: marco.verani@polimi.it

June 9, 2011

Abstract

In this paper we investigate the Mimetic Finite Difference method for the approximation of a constraint optimal control problem governed by an elliptic operator. *A priori* error estimates of the first order are derived in suitable discrete norms for both the control and the state variables. The theoretical results are confirmed by numerical experiments performed on a set of test cases selected from the literature.

Keywords optimal control problems, mimetic finite difference method, mixed formulation

1 Introduction

In recent years, there has been extensive research on the numerical approximation of optimal control problems that often arise in practical and industrial applications. Pioneering works on a priori error analysis of finite element approximation of quadratic elliptic optimal control problems can be found in [13, 14, 15]. Recently, this topic has seen an important renewal of interest (see e.g. the papers [2, 10, 20, 16], the books [17, 21] and the references therein).

More recently, a mixed finite element discretization for a general convex optimal control problem governed by elliptic equations has been analyzed in [11].

In this paper we investigate the Mimetic Finite Difference (MFD) method for the approximation of a constraint optimal control problem governed by an elliptic operator. This discretization technique can naturally deal with very general meshes which can be made of (possibly non convex) polyhedrals, and do not have to fulfill matching conditions. The MFD method can be interpreted as a generalization of the finite element method [8, 9] and, due to the great flexibility allowed in the mesh design, it has been rapidly applied to a wide range of problems (see [1, 3, 4, 5, 19], for example). However, its application to optimal control problems has not already been developed. Our main goal in this work is to perform such an investigation both theoretically and numerically.

The paper is organized as follows: in Section 2 we introduce the model problem, and we describe briefly its discretization by the Mimetic Finite Difference method. In Section 3 we derive error estimates in suitable mesh-dependent norms. Section 4 is devoted to present and discuss some numerical experiments on polygonal meshes in order to confirm our theoretical results. Finally, in Section 5 we draw some conclusion.

2 The optimal control problem and its mimetic discretization

Throughout the paper we will use standard notation for Sobolev spaces, norms and seminorms (see [12]).

Let Ω be an open, bounded, convex set of \mathbb{R}^2 , let K be a convex subset of $L^2(\Omega)$ and f a given function in $L^2(\Omega)$. We are interested in solving the following optimal control problem:

$$\begin{aligned} \min_{u \in K} \frac{1}{2} \int_{\Omega} (y - \bar{y})^2 + \frac{1}{2} \int_{\Omega} (F - \bar{F})^2 + \frac{\alpha}{2} \int_{\Omega} (u - \bar{u})^2, \\ -\Delta y = f + u \quad \text{in } \Omega, \\ y = 0 \quad \text{on } \partial\Omega \end{aligned} \tag{1}$$

where $\bar{y}, \bar{u} \in L^2(\Omega)$ and $\bar{F} \in [L^2(\Omega)]^d$ are given functions, $\alpha > 0$ and $F := -\nabla y$.

Let $X := H(\text{div}, \Omega) = \{G \in (L^2(\Omega))^d, \text{div}(G) \in L^2(\Omega)\}$, endowed with the norm of the graph given by

$$\|G\|_{\text{div}} := \|G\|_{H(\text{div}, \Omega)} = \left(\|G\|_{L^2(\Omega)}^2 + \|\text{div} G\|_{L^2(\Omega)}^2 \right)^{1/2},$$

and let $Q := L^2(\Omega)$. We consider the mixed formulation of problem (1): Find

$(F, y, u) \in X \times Q \times K$ such that

$$\begin{aligned} \min_{u \in K} \frac{1}{2} \int_{\Omega} (y - \bar{y})^2 + \frac{1}{2} \int_{\Omega} (F - \bar{F})^2 + \frac{\alpha}{2} \int_{\Omega} (u - \bar{u})^2, \\ (F, G) - (y, \operatorname{div} G) = 0 \quad \forall G \in X, \\ (\operatorname{div} F, q) = (f + u, q) \quad \forall q \in Q, \end{aligned} \quad (2)$$

where, here and in the following, (\cdot, \cdot) denotes the standard $L^2(\Omega)$ -inner product. It is well known [18] that problem (2) has a unique solution $(F, y, u) \in X \times Q \times K$ if and only if there exists $(P, z) \in X \times Q$ such that $(F, y, P, z, u) \in X \times Q \times X \times Q \times K$ satisfies the following optimality conditions:

$$\begin{aligned} (F, G) - (y, \operatorname{div} G) &= 0 & \forall G \in X, \\ (\operatorname{div} F, q) &= (f + u, q) & \forall q \in Q, \\ (P, G) - (z, \operatorname{div} G) &= -(F - \bar{F}, G) & \forall G \in X, \\ (\operatorname{div} P, q) &= (\bar{y} - y, q) & \forall q \in Q, \\ (\alpha(u - \bar{u}) - z, \tilde{u} - u) &\geq 0 & \forall \tilde{u} \in K. \end{aligned} \quad (3)$$

Next, we present a mimetic discretization of problem (3). Let $\Omega_h \subset \Omega$ be a polygonal approximation of Ω , in such a way that all vertexes of Ω_h which are on the boundary of Ω_h are also on the boundary of Ω . The polygonal domain Ω_h represents the computational domain.

With a little abuse of notation, we also denote by Ω_h a partition of the above introduced computational domain into polygons E . We assume that Ω_h is conformal, *i.e.*, intersection of two different polygons E_1 and E_2 is either a few mesh points, or a few mesh edges (two adjacent elements may share more than one edge) or empty. Elements $E \in \Omega_h$ are not required to be convex. For each polygon $E \in \Omega_h$, $|E|$ denotes its area, h_E denotes its diameter and

$$h := \max_{E \in \Omega_h} h_E.$$

We denote by \mathcal{N}_h and \mathcal{E}_h the sets of mesh vertexes and edges, by \mathcal{N}_h^0 and \mathcal{E}_h^0 the sets of internal vertexes and edges and by \mathcal{N}_h^∂ and \mathcal{E}_h^∂ the sets of boundary vertexes and edges, respectively. The sets of vertexes and edges of a particular element E are denoted by \mathcal{N}_h^E and \mathcal{E}_h^E , respectively. Moreover, we refer to a generic mesh vertex by \mathbf{v} , a generic edge by \mathbf{e} and denote its length $|\mathbf{e}|$.

A fixed orientation is also set for the mesh Ω_h , which is reflected by a unit normal vector $\mathbf{n}_\mathbf{e}$, $\mathbf{e} \in \mathcal{E}_h$, fixed once and for all. For every polygon E and edge $\mathbf{e} \in \mathcal{E}_h^E$, we define a unit normal vector $\mathbf{n}_E^\mathbf{e}$ that points outside of E .

The mesh is assumed to satisfy the following shape regularity properties, which have already been used in [9]:

- (M1) There exists a positive integer $N_\mathbf{e}$ such that every element E has at most $N_\mathbf{e}$ edges.

(M2) There exists a positive number τ such that every element E is star-shaped with respect to every point of a ball centered at $C_E \in E$ and with radius τh_E .

(M3) There exists a positive constant γ such that for any element E and for every edge \mathbf{e} of E it holds $|\mathbf{e}| \geq \gamma h_E$.

To approximate the mixed problem (3) we introduce the linear spaces of discrete fields, denoted by Q^d and X^d , respectively representing the degrees of freedom of the scalar variable and the flux. We associate the degrees of freedom of the scalar variable to mesh cells so that for $\mathbf{q} \in Q^d$ we have $\mathbf{q} = \{q_E\}_{E \in \Omega_h}$, with $q_E \in \mathbb{R}$. Flux degrees of freedom are associated to mesh faces so that for $\mathbf{G} \in X^d$, we have $\mathbf{G} = \{G_E^{\mathbf{e}}\}_{\mathbf{e} \in \partial E}$, with $G_E^{\mathbf{e}} \in \mathbb{R}$ with the additional assumption of normal flux continuity, i.e.,

$$G_{E_1}^{\mathbf{e}} + G_{E_2}^{\mathbf{e}} = 0 ,$$

when $\bar{\mathbf{e}} = \bar{E}_1 \cap \bar{E}_2$, $E_1, E_2 \in \Omega_h$. It is clear that the dimension of Q^d equals the number of mesh cells, and the dimension of X^d equals the number of mesh faces. We also introduce two interpolation operators for $q \in L^1(\Omega)$ and $G \in H(\text{div}, \Omega)$, respectively. In particular, for every $E \in \Omega_h$ and $\mathbf{e} \subseteq \partial E$ we set

$$(\mathbf{q}^I)_E := \frac{1}{|E|} \int_E q \, dV , \quad (\mathbf{G}^I)_E^{\mathbf{e}} := \frac{1}{|\mathbf{e}|} \int_{\mathbf{e}} \mathbf{n}_E^{\mathbf{e}} \cdot G \, dS .$$

We equip the spaces Q^d and X^d with two suitable scalar products. We define the scalar product in Q^d as

$$[\mathbf{p}, \mathbf{q}]_{Q^d} := \sum_{E \in \Omega_h} |E| p_E q_E \quad \forall \mathbf{p}, \mathbf{q} \in Q^d , \quad (4)$$

which corresponds to the $L^2(\Omega)$ scalar product for piecewise constant functions. The scalar product in X^d is defined by assembling the elementwise contributions from each element

$$[\mathbf{F}, \mathbf{G}]_{X^d} := \sum_{E \in \Omega_h} [\mathbf{F}, \mathbf{G}]_E \quad \forall \mathbf{F}, \mathbf{G} \in X^d . \quad (5)$$

The local scalar product $[\cdot, \cdot]_E$ on $X^d|_E$ is required to satisfy the following two conditions:

(S1) Stability: there exists two positive constants C_1 and C_2 independent of h such that

$$C_1 \sum_{\mathbf{e} \in \partial E} |E| (G_E^{\mathbf{e}})^2 \leq [\mathbf{G}, \mathbf{G}]_E \leq C_2 \sum_{\mathbf{e} \in \partial E} |E| (G_E^{\mathbf{e}})^2$$

for all $\mathbf{G} \in X^d$ and for every element $E \in \Omega_h$;

(S2) Local consistency: for every linear function q^1 on $E \in \Omega_h$ it holds

$$[(\nabla q^1)^I, \mathbf{G}]_E + \int_E q^1 \mathcal{D}\mathcal{I}\mathcal{V}_h \mathbf{G} \, dV = \sum_{e \in \partial E} G_E^e \int_e q^1 \, dS$$

for all $\mathbf{G} \in X^d$.

Here the mimetic discrete divergence operator $\mathcal{D}\mathcal{I}\mathcal{V}^d : X^d \rightarrow Q^d$ is defined elementwise as:

$$(\mathcal{D}\mathcal{I}\mathcal{V}^d \mathbf{G})_E := \frac{1}{|E|} \sum_{e \in \partial E} |e| G_E^e,$$

for $\mathbf{G} \in X^d$ and $E \in \Omega_h$. This definition is consistent with the Gauss divergence theorem. Moreover, it holds

$$(\operatorname{div} G)^I = \mathcal{D}\mathcal{I}\mathcal{V}^d(\mathbf{G}^I) \quad \forall G \in X.$$

The mimetic divergence operator is naturally associated to the discrete flux operator $\mathcal{G}^d : Q^d \rightarrow X^d$ defined by:

$$[\mathbf{G}, \mathcal{G}^d \mathbf{q}]_{X^d} := -[\mathcal{D}\mathcal{I}\mathcal{V}^d \mathbf{G}, \mathbf{q}]_{Q^d} \quad \forall \mathbf{q} \in Q^d, \mathbf{G} \in X^d.$$

Finally, let $K^d \subseteq Q^d$ be a closed subset of Q^d . So, the mimetic discretization of (3) reads as follows: Find $(\mathbf{F}_d, \mathbf{y}_d, \mathbf{P}_d, \mathbf{z}_d, \mathbf{u}_d) \in X^d \times Q^d \times X^d \times Q^d \times K^d$ such that

$$\begin{aligned} [\mathbf{F}_d, \mathbf{G}]_{X^d} - [\mathbf{y}_d, \mathcal{D}\mathcal{I}\mathcal{V}^d \mathbf{G}]_{Q^d} &= 0 & \forall \mathbf{G} \in X^d, \\ [\mathcal{D}\mathcal{I}\mathcal{V}^d \mathbf{F}_d, \mathbf{q}]_{Q^d} &= [\mathbf{f} + \mathbf{u}_d, \mathbf{q}]_{Q^d} & \forall \mathbf{q} \in Q^d, \\ [\mathbf{P}_d, \mathbf{G}]_{X^d} - [\mathbf{z}_d, \mathcal{D}\mathcal{I}\mathcal{V}^d \mathbf{G}]_{Q^d} &= -[\mathbf{F}_d - \bar{\mathbf{F}}, \mathbf{G}]_{X^d} & \forall \mathbf{G} \in X^d, \\ [\mathcal{D}\mathcal{I}\mathcal{V}^d \mathbf{P}_d, \mathbf{q}]_{Q^d} &= [\bar{\mathbf{y}} - \mathbf{y}_d, \mathbf{q}]_{Q^d} & \forall \mathbf{q} \in Q^d, \\ [\alpha(\mathbf{u}_d - \bar{\mathbf{u}}) - \mathbf{z}_d, \tilde{\mathbf{u}} - \mathbf{u}_d]_{Q^d} &\geq 0 & \forall \tilde{\mathbf{u}} \in K^d, \end{aligned} \quad (6)$$

where $\mathbf{f} = \mathbf{f}^I$, $\bar{\mathbf{y}} = \bar{\mathbf{y}}^I$, $\bar{\mathbf{F}} = \bar{\mathbf{F}}^I$ and $\bar{\mathbf{u}} = \bar{\mathbf{u}}^I$ are the vectors of the mean values of f , \bar{y} , \bar{F} and of \bar{u} , respectively. In the next section we derive *a priori* error estimates in the discrete norms (4) and (5) for the pressure and the flux variables.

3 Convergence analysis

In the following we assume $K^d \subseteq K$, and we use the symbol \lesssim to indicate an upper bound that holds up to a positive multiplicative constant independent of h . Furthermore, for the ease of presentation, we shall use bold letters to denote both the generic element of Q^d and the corresponding piecewise constant function defined on Ω_h . Accordingly, the scalar products will be identified, i.e., $(\mathbf{u}, \mathbf{q})_{L^2(\Omega)} = [\mathbf{u}, \mathbf{q}]_{Q^d}$ for all $\mathbf{u}, \mathbf{q} \in Q^d$.

Let us first introduce two intermediate problems, that will be useful in the

forthcoming analysis. Let $\mathbf{v}_d \in Q^d$, the first intermediate problem reads as follows: Find $(F(\mathbf{v}_d), y(\mathbf{v}_d)) \in X \times Q$ such that

$$\begin{aligned} (F(\mathbf{v}_d), G) - (y(\mathbf{v}_d), \operatorname{div} G) &= 0 & \forall G \in X, \\ (\operatorname{div} F(\mathbf{v}_d), q) &= (f + \mathbf{v}_d, q) & \forall q \in Q. \end{aligned} \quad (7)$$

The second intermediate problem reads as follows: Find $(P(\mathbf{v}_d), z(\mathbf{v}_d)) \in X \times Q$ such that

$$\begin{aligned} (P(\mathbf{v}_d), G) - (z(\mathbf{v}_d), \operatorname{div} G) &= -(F - \bar{F}, G) & \forall G \in X, \\ (\operatorname{div} P(\mathbf{v}_d), q) &= (\bar{y} - y(\mathbf{v}_d), q) & \forall q \in Q, \end{aligned} \quad (8)$$

where $y(\mathbf{v}_d)$ is the solution of (7).

We are now ready to state the main result of this paper.

Theorem 3.1 *Let $(F, y, P, z, u) \in X \times Q \times X \times Q \times K$ be the exact optimal solution to (3) and $(\mathbf{F}_d, \mathbf{y}_d, \mathbf{P}_d, \mathbf{z}_d, \mathbf{u}_d) \in X^d \times Q^d \times X^d \times Q^d \times K^d$ be the discrete optimal solution to (6). Then,*

$$\|\mathbf{u}^I - \mathbf{u}_d\|_{Q^d} \lesssim h \quad (9)$$

and

$$\|\mathbf{F}^I - \mathbf{F}_d\|_{X^d} + \|\mathbf{y}^I - \mathbf{y}_d\|_{Q^d} \lesssim h, \quad (10)$$

$$\|\mathbf{P}^I - \mathbf{P}_d\|_{X^d} + \|\mathbf{z}^I - \mathbf{z}_d\|_{Q^d} \lesssim h. \quad (11)$$

Proof. Let us first prove (9). By using the triangle inequality together with standard interpolation error estimates (see [7] for more details), we get

$$\|\mathbf{u}^I - \mathbf{u}_d\|_{Q^d} \leq \|\mathbf{u}^I - u\|_{L^2(\Omega)} + \|u - \mathbf{u}_d\|_{L^2(\Omega)} \lesssim h + \|u - \mathbf{u}_d\|_{L^2(\Omega)}.$$

Hence, we reduce ourselves to estimate $\|u - \mathbf{u}_d\|_{L^2(\Omega)}$. Taking $\tilde{u} = \mathbf{u}_d$ in the last inequality in (3), and $\tilde{\mathbf{u}} = \mathbf{u}^I$ in the last inequality in (6) yields

$$(\alpha(u - \tilde{u}) - z, \mathbf{u}_d - u) \geq 0, \quad (12)$$

$$(\alpha(\mathbf{u}_d - \tilde{\mathbf{u}}) - \mathbf{z}_d, \mathbf{u}^I - \mathbf{u}_d) \geq 0. \quad (13)$$

By using the simple fact that $\mathbf{u}^I - \mathbf{u}_d = \mathbf{u}^I - u + u - \mathbf{u}_d$ and adding (12)-(13), we have

$$0 \leq (\alpha(\mathbf{u}_d - \tilde{\mathbf{u}}) - \mathbf{z}_d, \mathbf{u}^I - u) + (\alpha(\mathbf{u}_d - u) + \alpha(\tilde{u} - \tilde{\mathbf{u}}) + (z - \mathbf{z}_d), u - \mathbf{u}_d).$$

Hence, there follows

$$\begin{aligned}
\alpha \|u - \mathbf{u}_d\|_{L^2(\Omega)}^2 &\leq (\alpha(\mathbf{u}_d - \bar{\mathbf{u}}) - \mathbf{z}_d, \mathbf{u}^I - u) + (\alpha(\bar{u} - \bar{\mathbf{u}}) + (z - \mathbf{z}_d), u - \mathbf{u}_d) \\
&= (\alpha(u - \bar{u}) - z, \mathbf{u}^I - u) + \alpha(\mathbf{u}_d - u, \mathbf{u}^I - u) \\
&\quad + \alpha(\bar{u} - \bar{\mathbf{u}}, \mathbf{u}^I - u) + (z - \mathbf{z}_d, \mathbf{u}^I - u) + \alpha(\bar{u} - \bar{\mathbf{u}}, u - \mathbf{u}_d) \\
&\quad + (z - z(\mathbf{u}_d), u - \mathbf{u}_d) + (z(\mathbf{u}_d) - \mathbf{z}_d, u - \mathbf{u}_d) \\
&= (\alpha(u - \bar{u}) - z, \mathbf{u}^I - u) + \alpha(\mathbf{u}_d - u, \mathbf{u}^I - u) \\
&\quad + \alpha(\bar{u} - \bar{\mathbf{u}}, \mathbf{u}^I - u) + (z - z(\mathbf{u}_d), \mathbf{u}^I - u) \\
&\quad + (z(\mathbf{u}_d) - \mathbf{z}_d, \mathbf{u}^I - u) + \alpha(\bar{u} - \bar{\mathbf{u}}, u - \mathbf{u}_d) \\
&\quad + (z - z(\mathbf{u}_d), u - \mathbf{u}_d) + (z(\mathbf{u}_d) - \mathbf{z}_d, u - \mathbf{u}_d) \\
&:= I + II + III + IV + V + VI + VII + VIII . \tag{14}
\end{aligned}$$

Let us analyze the terms $I - VIII$ separately.

The terms I , III and VI can be estimated by using regularity results for elliptic equations and standard interpolation results, as follows

$$\begin{aligned}
I &= (\alpha(u - \bar{u}) - z, \mathbf{u}^I - u) \leq \|\alpha(u - \bar{u}) - z\|_{H^1(\Omega)} \|\mathbf{u}^I - u\|_{H^{-1}(\Omega)} \lesssim h^2, \\
III &= \alpha(\bar{u} - \bar{\mathbf{u}}, \mathbf{u}^I - u) \leq \alpha \|\bar{u} - \bar{\mathbf{u}}\|_{L^2(\Omega)} \|\mathbf{u}^I - u\|_{L^2(\Omega)} \lesssim h^2, \\
VI &= \alpha(\bar{u} - \bar{\mathbf{u}}, u - \mathbf{u}_d) \leq \alpha \|\bar{u} - \bar{\mathbf{u}}\|_{L^2(\Omega)} \|u - \mathbf{u}_d\|_{L^2(\Omega)} \lesssim h \|u - \mathbf{u}_d\|_{L^2(\Omega)}.
\end{aligned}$$

Then the Young inequality yields, for $\epsilon > 0$, to

$$II = \alpha(\mathbf{u}_d - u, \mathbf{u}^I - u) \leq \frac{\alpha^2}{2\epsilon} \|u - \mathbf{u}_d\|_{L^2(\Omega)}^2 + \frac{\epsilon}{2} \|\mathbf{u}^I - u\|_{L^2(\Omega)}^2 .$$

In order to estimate the term IV in (14) we observe that thanks to the Cauchy-Schwarz inequality and the regularity results for elliptic equations (7) and (8), we have

$$\begin{aligned}
IV = (z - z(\mathbf{u}_d), \mathbf{u}^I - u) &\leq \|z(u) - z(\mathbf{u}_d)\|_{H^1(\Omega)} \|\mathbf{u}^I - u\|_{L^2(\Omega)} \\
&\lesssim h \|y(u) - y(\mathbf{u}_d)\|_{H^1(\Omega)} \\
&\lesssim h \|u - \mathbf{u}_d\|_{L^2(\Omega)} .
\end{aligned}$$

Proceeding as before and taking into account [8, Theorem 5.3], we get

$$\begin{aligned}
V = (z(\mathbf{u}_d) - \mathbf{z}_d, \mathbf{u}^I - u) &\leq \|z(\mathbf{u}_d) - \mathbf{z}_d\|_{L^2(\Omega)} \|\mathbf{u}^I - u\|_{L^2(\Omega)} \\
&\lesssim h (\|z(\mathbf{u}_d) - \mathbf{z}(\mathbf{u}_d)^I\|_{L^2(\Omega)} + \|\mathbf{z}(\mathbf{u}_d)^I - \mathbf{z}_d\|_{L^2(\Omega)}) \\
&\lesssim h^2 .
\end{aligned}$$

Now, let us estimate the term VII . By using (7) and (8), it is easy to check that the following relations hold

$$(f + u, z(u)) = (\bar{y} - y(u), y(u)) , \tag{15}$$

$$(f + u, z(\mathbf{u}_d)) = (\bar{y} - y(\mathbf{u}_d), y(u)) , \tag{16}$$

$$(f + \mathbf{u}_d, z(u)) = (\bar{y} - y(u), y(\mathbf{u}_d)) , \tag{17}$$

$$(f + \mathbf{u}_d, z(\mathbf{u}_d)) = (\bar{y} - y(\mathbf{u}_d), y(\mathbf{u}_d)) . \tag{18}$$

By subtracting (16) from (15) and subtracting (18) from (17), we get

$$\begin{aligned} (f, z(u) - z(\mathbf{u}_d)) + (u, z(u) - z(\mathbf{u}_d)) &= (y(\mathbf{u}_d) - y(u), y(u)) , \\ (f, z(u) - z(\mathbf{u}_d)) + (\mathbf{u}_d, z(u) - z(\mathbf{u}_d)) &= (y(\mathbf{u}_d) - y(u), y(\mathbf{u}_d)) . \end{aligned} \quad (19)$$

By subtracting (19) from (19) we obtain

$$VII = (z(u) - z(\mathbf{u}_d), u - \mathbf{u}_d) = (y(\mathbf{u}_d) - y(u), y(u) - y(\mathbf{u}_d)) \leq 0 . \quad (20)$$

Finally, the Cauchy-Schwarz inequality together with [8, Theorem 5.3] and standard interpolation results yield to

$$\begin{aligned} VIII &= (z(\mathbf{u}_d) - \mathbf{z}_d, u - \mathbf{u}_d) \\ &\leq (\|z(\mathbf{u}_d) - \mathbf{z}(\mathbf{u}_d)^I\|_{L^2(\Omega)} + \|\mathbf{z}(\mathbf{u}_d)^I - \mathbf{z}_d\|_{L^2(\Omega)}) \|u - \mathbf{u}_d\|_{L^2(\Omega)} \\ &\lesssim h \|u - \mathbf{u}_d\|_{L^2(\Omega)} . \end{aligned}$$

Then, (9) follows collecting all the previous estimates.

We next estimate $\|\mathbf{F}^I - \mathbf{F}_d\|_{X^d}$. By using the triangle inequality we have

$$\|\mathbf{F}^I - \mathbf{F}_d\|_{X^d} \leq \|\mathbf{F}(u)^I - \mathbf{F}(\mathbf{u}_d)^I\|_{X^d} + \|\mathbf{F}(\mathbf{u}_d)^I - \mathbf{F}_d\|_{X^d} ,$$

where $\mathbf{F}(u) = \mathbf{F}$ and $\mathbf{F}(\mathbf{u}_d)$ are the solutions of the intermediate problem (7). By employing [8, Lemma 4.1], equations (3) and (7) together with classical regularity results for elliptic equations we have

$$\begin{aligned} \|(\mathbf{F} - \mathbf{F}(\mathbf{u}_d))^I\|_{X^d}^2 &\leq \|\mathbf{F}(u) - \mathbf{F}(\mathbf{u}_d)\|_{[L^2(\Omega)]^d}^2 + \sum_{E \in \Omega_h} h_E^2 \|\operatorname{div}(\mathbf{F}(u) - \mathbf{F}(\mathbf{u}_d))\|_{L^2(E)}^2 \\ &\leq \|y(u) - y(\mathbf{u}_d)\|_{H^1(\Omega)}^2 + \sum_{E \in \Omega_h} h_E^2 \|u - \mathbf{u}_d\|_{L^2(E)}^2 \\ &\leq \|u - \mathbf{u}_d\|_{L^2(\Omega)}^2 + \sum_{E \in \Omega_h} h_E^2 \|u - \mathbf{u}_d\|_{L^2(E)}^2 \\ &\leq \|u - \mathbf{u}^I\|_{L^2(\Omega)}^2 + \|\mathbf{u}^I - \mathbf{u}_d\|_{L^2(\Omega)}^2 + \sum_{E \in \Omega_h} h_E^2 \|u - \mathbf{u}_d\|_{L^2(E)}^2 . \end{aligned}$$

Then, thanks to (9) and standard interpolation results, we get $\|(\mathbf{F} - \mathbf{F}(\mathbf{u}_d))^I\|_{X^d} \lesssim h$. Moreover, [8, Theorem 5.2] yields to $\|\mathbf{F}(\mathbf{u}_d)^I - \mathbf{F}_d\|_{X^d} \lesssim h$. Hence, it follows $\|\mathbf{F}^I - \mathbf{F}_d\|_{X^d} \lesssim h$.

Next we estimate $\|\mathbf{y}^I - \mathbf{y}_d\|_{Q^d}$. By using the triangle inequality, we have

$$\|\mathbf{y}^I - \mathbf{y}_d\|_{Q^d} \leq \|(y(u) - \mathbf{y}(\mathbf{u}_d))^I\|_{L^2(\Omega)} + \|\mathbf{y}(\mathbf{u}_d)^I - \mathbf{y}_d\|_{L^2(\Omega)} .$$

By employing the continuity of the interpolation operator, we get

$$\|\mathbf{y}^I - \mathbf{y}_d\|_{Q^d} \leq \|y(u) - y(\mathbf{u}_d)\|_{L^2(\Omega)} + \|\mathbf{y}(\mathbf{u}_d)^I - \mathbf{y}_d\|_{L^2(\Omega)} .$$

Finally, using regularity results for elliptic equations together with [8, Theorem 5.3] it follows

$$\begin{aligned} \|\mathbf{y}^I - \mathbf{y}_d\|_{Q^d} &\lesssim \|u - \mathbf{u}_d\|_{L^2(\Omega)} + h \\ &\lesssim \|u - \mathbf{u}^I\|_{L^2(\Omega)} + \|\mathbf{u}^I - \mathbf{u}_d\|_{L^2(\Omega)} + h \\ &\lesssim h, \end{aligned}$$

where in the last step we employed a standard interpolation result together with (9). This concludes the proof of (10). In the same way it is possible to prove (11). \square

Remark 3.1 *A similar a priori analysis holds also in the case of the lowest order Raviart-Thomas elements as demonstrated in [11, Theorem 4.1]. However this result cannot be directly applied to the MFD method because the two numerical methods coincide only in the case of triangular meshes and for a particular choice of the local scalar product involved in (5). See [9] for more details.*

4 Numerical experiments

The numerical experiments presented in this section aim to confirm the *a priori* analysis contained in Section 4. The optimization problem is solved numerically by using the Primal-Dual strategy (see [6] for more details). We test our numerical algorithm on four examples: the first two test cases are taken from [11]; two variants of them are performed in test cases 3 and 4, and have been considered in order to investigate how the configuration of the interior boundary of the active region influences the performance of the numerical method. We

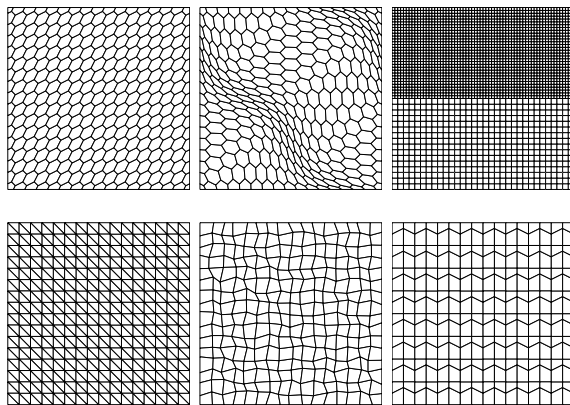


Figure 1: Examples of the considered decompositions of $\Omega =]0, 1[^2$. From left to right: *hexagons-type 1, hexagons-type 2, non-matching quadrilaterals; triangles, quadrilaterals and trapezes.*

consider six different sequences of decomposition of the domain $\Omega =]0, 1[^2$, that

we denote by *hexagons-type 1*, *hexagons-type 2*, *non-matching quadrilaterals*, *triangles*, *quadrilaterals* and *trapezes*. An example of all the considered decompositions is shown in Figure 1. It is worth noting that also non conforming grids are permitted.

4.1 Test Case 1

In the first test, we solve problem (3) setting

$$\begin{aligned} f &= 2\pi^2 y - u, & \bar{u} &= 1 - \sin(\pi x_1/2) - \sin(\pi x_2/2), \\ \bar{y} &= (1 - 2\pi^2)y, & \bar{\mathbf{F}} &= \begin{pmatrix} -\pi \cos(\pi x_1) \sin(\pi x_2) \\ -\pi \sin(\pi x_1) \cos(\pi x_2) \end{pmatrix}, \end{aligned}$$

where y, p, u are the exact solutions given by:

$$y = \sin(\pi x_1) \sin(\pi x_2), \quad z = -\sin(\pi x_1) \sin(\pi x_2), \quad u = \max(\bar{u} + z, 0).$$

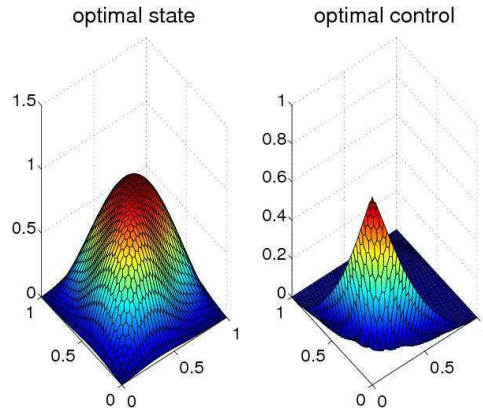


Figure 2: Test Case 1. Computed optimal state (left) and optimal control (right).

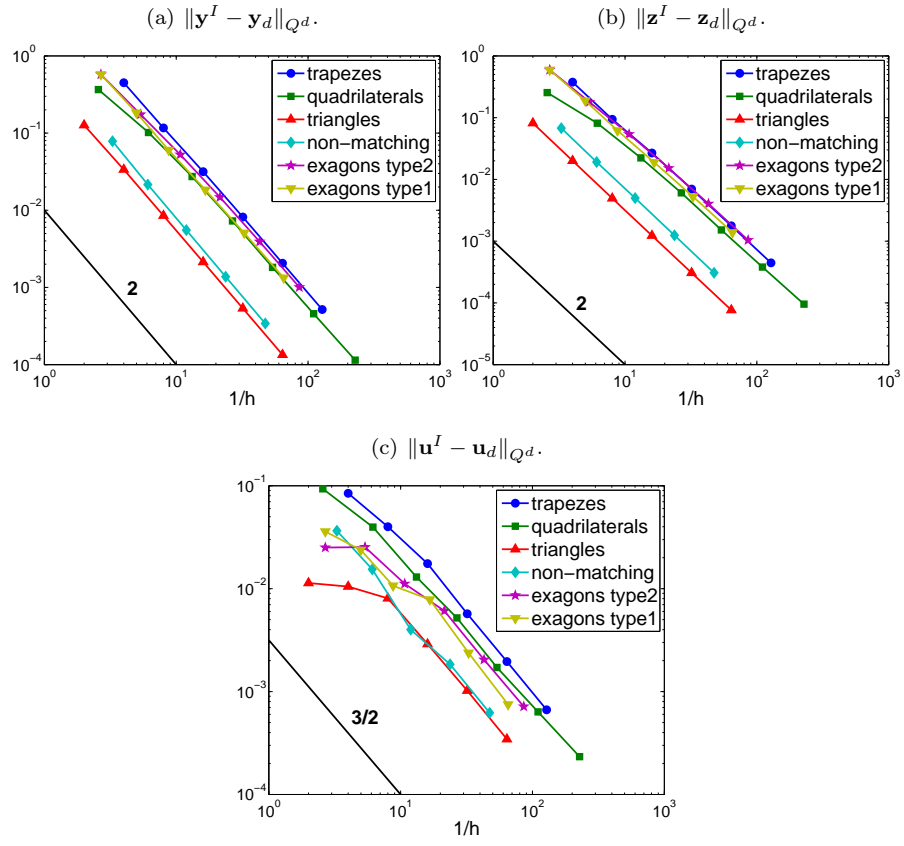


Figure 3: Test Case 1. Computed errors $\|\mathbf{y}^I - \mathbf{y}_d\|_{Q^d}$, $\|\mathbf{z}^I - \mathbf{z}_d\|_{Q^d}$, $\|\mathbf{u}^I - \mathbf{u}_d\|_{Q^d}$ versus $1/h$ (loglog scale).

An example of the computed optimal state and optimal control is shown in Figure 2. In Figure 3 (loglog scale) we report the computed errors in the discrete energy norm defined in (4): for all the mesh configuration we observe a quadratic convergence rate for the primal variable y and for the dual variable p , whereas the error in control variable u seems to go to zero at a rate of $3/2$ as the mesh-size h goes to zero. We observe that in all the test cases convergence is achieved at a slightly better rate than predicted by our theoretical analysis.

4.2 Test Case 2

In the second test we choose as exact solutions

$$y = \sin(\pi x_1) \sin(\pi x_2), \quad z = -\sin(2\pi x_1) \sin(2\pi x_2), \quad u = \max(\bar{u} + z, 0),$$

and set in problem (3)

$$f = 2\pi^2 y - u, \quad \bar{u} = 0.7, \quad \bar{y} = y, \\ \bar{\mathbf{F}} = \begin{pmatrix} -\pi \cos(\pi x_1) \sin(\pi x_2) - 2\pi \cos(2\pi x_1) \sin(2\pi x_2) \\ -\pi \sin(\pi x_1) \cos(\pi x_2) - 2\pi \sin(2\pi x_1) \cos(2\pi x_2) \end{pmatrix}.$$

Figure 4 shows the computed optimal state and control on a *hexagons-type 2* decomposition. In Figure 5 (loglog scale) we report the computed errors in the

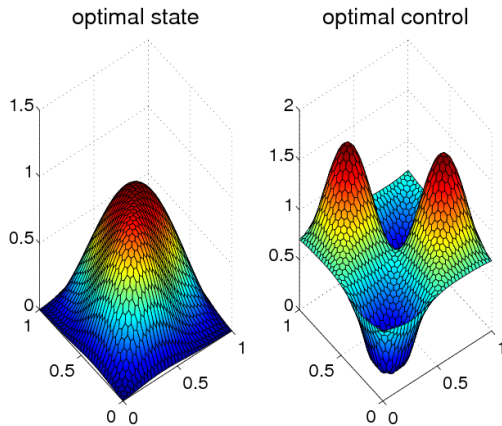


Figure 4: Test Case 2. Computed optimal state (left) and optimal control (right).

discrete energy norm defined in (4). We observe a quadratic convergence rate for the primal variable y , for the dual variable p and for the control. Note that in this case the control variable converges slightly better than in test case 1.

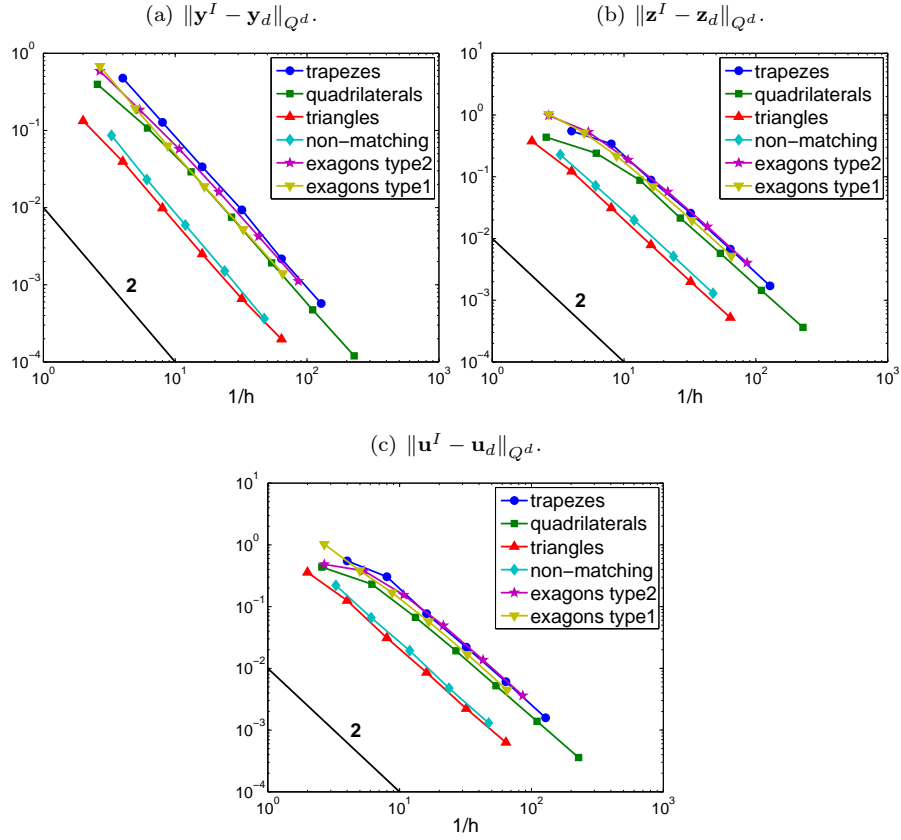


Figure 5: Test Case 2. Computed errors $\|\mathbf{y}^I - \mathbf{y}_d\|_{Q^d}$, $\|\mathbf{z}^I - \mathbf{z}_d\|_{Q^d}$, $\|\mathbf{u}^I - \mathbf{u}_d\|_{Q^d}$ versus $1/h$ (loglog scale).

4.3 Test Case 3

The third example is a variant of the test case 1. Our aim is to analyze how the interior boundary of the active region influences the behaviour of the error. For this reason, we choose as exact solutions of problem (3)

$$y = 5\pi^2 \sin(\pi x_1) \sin(2\pi x_2), \quad z = -\sin(\pi x_1) \sin(2\pi x_2), \quad u = \max(\bar{u} + z, 0),$$

and set

$$f = 25\pi^4 y - u, \quad \bar{u} = 0, \quad \bar{y} = 0,$$

$$\bar{\mathbf{F}} = \begin{pmatrix} -5\pi^3 \cos(\pi x_1) \sin(2\pi x_2) \\ -10\pi^3 \sin(\pi x_1) \cos(2\pi x_2) \end{pmatrix}.$$

A sample of the computed optimal state and optimal control is shown in Figure 6. Observe that the interior boundary of the active region is a straight line; so

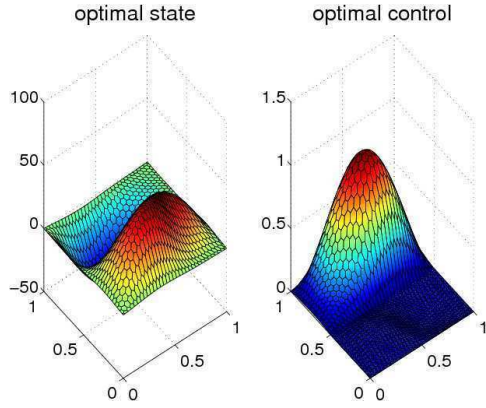


Figure 6: Test Case 3. Computed optimal state (left) and optimal control (right).

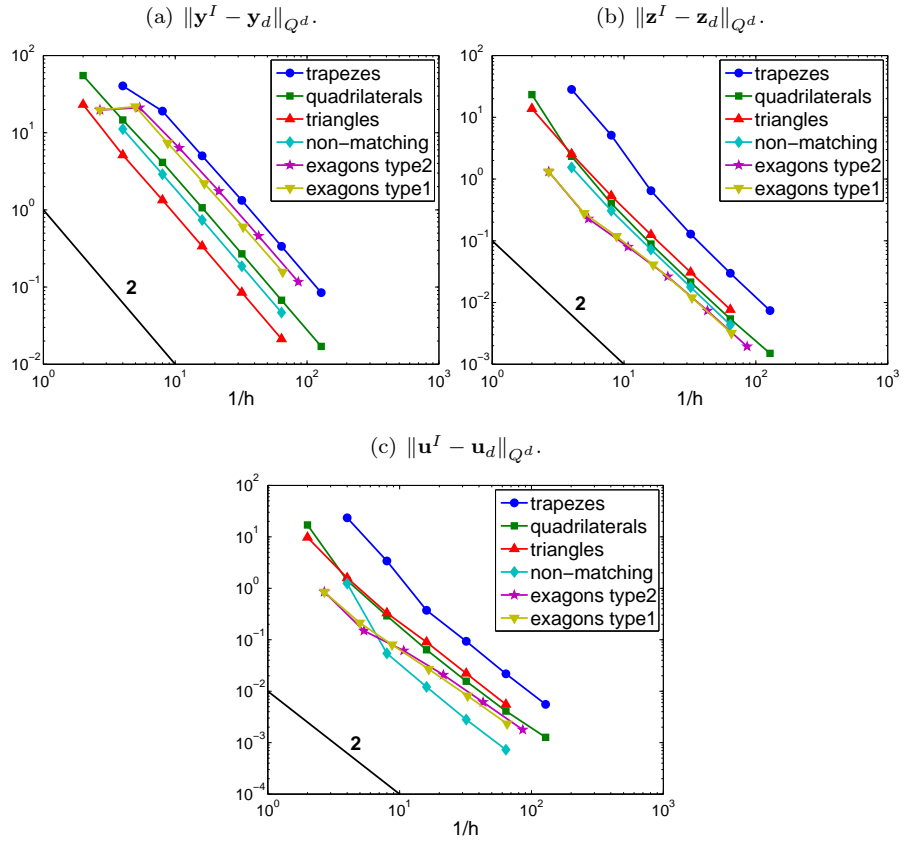


Figure 7: Test Case 3. Computed errors $\|\mathbf{y}^I - \mathbf{y}_d\|_{Q^d}$, $\|\mathbf{z}^I - \mathbf{z}_d\|_{Q^d}$, $\|\mathbf{u}^I - \mathbf{u}_d\|_{Q^d}$ versus $1/h$ (log scale).

it is aligned with most of the decompositions shown in Figure 1. In Figure 7 we report the computed errors for both the primal, the dual and the control variables. In all the cases, the errors go to zero quadratically as the mesh is refined.

4.4 Test Case 4

In the last example we solve (3) setting

$$\begin{aligned} f &= 2\pi^2 y - u, & \bar{u} &= \exp(x_1^2 + x_2^2) \sin(5\pi x_1) + \sin(5\pi x_2), \\ \bar{y} &= (1 - 2\pi^2)y, & \bar{\mathbf{F}} &= \begin{pmatrix} -\pi \cos(\pi x_1) \sin(\pi x_2) \\ -\pi \sin(\pi x_1) \cos(\pi x_2) \end{pmatrix}, \end{aligned}$$

where y, p, u are the exact solutions given by:

$$y = \sin(\pi x_1) \sin(\pi x_2), \quad z = -\sin(\pi x_1) \sin(\pi x_2), \quad u = \max(\bar{u} + z, 0).$$

In this case the configuration of the interior boundary separating the active region and the inactive one is more complicated. We can see this fact in Figure 8 (right), where an example of the discrete optimal state and of the optimal control is shown. In Figure 9 (loglog scale) we report the computed errors in

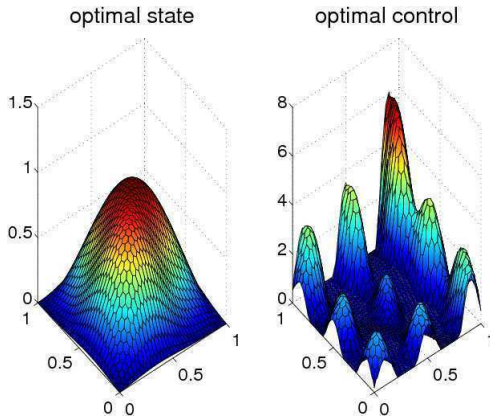


Figure 8: Test Case 4. Computed optimal state (left) and optimal control (right).

the discrete energy norm (4). We observe a quadratic convergence rate for the primal variable y and for the dual variable p , while the error of the control variable converges to zero at a rate of $3/2$, as the mesh-size goes to zero.

Remark 4.1 *We can observe that our a priori analysis is confirmed by all the numerical examples. However, the computed errors seem to converge better than expected. Such a behaviour is referred as superconvergence effect and has already*

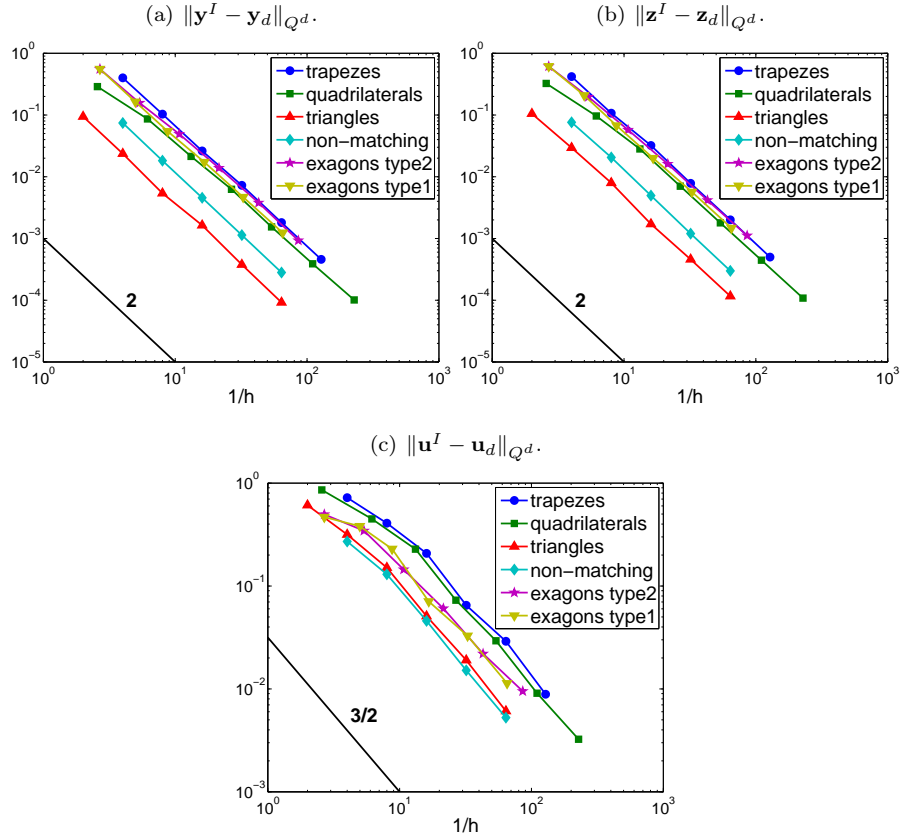


Figure 9: Test Case 4. Computed errors $\|\mathbf{y}^I - \mathbf{y}_d\|_{Q^d}$, $\|\mathbf{z}^I - \mathbf{z}_d\|_{Q^d}$, $\|\mathbf{u}^I - \mathbf{u}_d\|_{Q^d}$ versus $1/h$ (loglog scale).

been observed in [11] for a similar problem. In [11, Lemma 5.1, Theorem 5.1] a proof of this behaviour for the case of the lowest order Raviart-Thomas elements is presented. With regard to the MFD method a theoretical justification is still under investigation and will be object of future research.

5 Conclusions.

We proposed a Mimetic Finite Difference discretization of a quadratic control problem governed by an elliptic equation. The method is presented on polygonal decompositions made by general-shaped elements. *A priori* error estimates for both the control and the state variables are shown. Our error analysis has been confirmed by the numerical examples where a superconvergence behaviour has also been observed.

References

- [1] P. Antonietti, L. Beirão da Veiga, and M. Verani. A mimetic discretization of elliptic obstacle problems. Technical Report 14, MOX, Dipartimento di Matematica, Politecnico di Milano, 2010. <http://mox.polimi.it/it/progetti/pubblicazioni/>.
- [2] N. Arada, E. Casas, and F. Tröltzsch. Error estimates for the numerical approximation of a semilinear elliptic control problem. *Comput. Optim. Appl.*, 23(2):201–229, 2002.
- [3] L. Beirão da Veiga, V. Gyrya, K. Lipnikov, and G. Manzini. Mimetic finite difference method for the Stokes problem on polygonal meshes. *J. Comput. Phys.*, 228(19):7215–7232, 2009.
- [4] L. Beirão da Veiga and D. Mora. A mimetic discretization of the Reissner-Mindlin plate bending problem. *Numerische Mathematik*, 117:425–462, 2011. 10.1007/s00211-010-0358-8.
- [5] L. Beirão Da Veiga. A mimetic discretization method for linear elasticity. *M2AN Math. Model. Numer. Anal.*, 44(2):231–250, 2010.
- [6] M. Bergounioux, K. Ito, and K. Kunisch. Primal-dual strategy for constrained optimal control problems. *SIAM J. Control Optim.*, 37(4):1176–1194 (electronic), 1999.
- [7] S. Brenner and L. Scott. *The Mathematical Theory of Finite Element Methods*. Springer-Verlag, Berlin/Heidelberg, 1994.
- [8] F. Brezzi, K. Lipnikov, and M. Shashkov. Convergence of the mimetic finite difference method for diffusion problems on polyhedral meshes. *SIAM J. Numer. Anal.*, 43(5):1872–1896, 2005.
- [9] F. Brezzi, K. Lipnikov, and V. Simoncini. A family of mimetic finite difference methods on polygonal and polyhedral meshes. *Math. Models Methods Appl. Sci.*, 15(10):1533–1551, 2005.
- [10] E. Casas and F. Tröltzsch. Error estimates for linear-quadratic elliptic control problems. In *Analysis and optimization of differential systems (Constanta, 2002)*, pages 89–100. Kluwer Acad. Publ., Boston, MA, 2003.
- [11] Y. Chen, Y. Huang, W. Liu, and N. Yan. Error estimates and superconvergence of mixed finite element methods for convex optimal control problems. *J. Sci. Comput.*, 42(3):382–403, 2010.
- [12] G. Evans, J. Blackledge, and P. Yardley. *Numerical methods for partial differential equations*. Springer Undergraduate Mathematics Series. Springer-Verlag London Ltd., London, 2000.
- [13] R. S. Falk. Approximation of a class of optimal control problems with order of convergence estimates. *J. Math. Anal. Appl.*, 44:28–47, 1973.

- [14] R. S. Falk. Error estimates for the approximation of a class of variational inequalities. *Math. Comput.*, 28:963–971, 1974.
- [15] T. Geveci. On the approximation of the solution of an optimal control problem governed by an elliptic equation. *RAIRO Anal. Numér.*, 13(4):313–328, 1979.
- [16] M. Hinze. A variational discretization concept in control constrained optimization: the linear-quadratic case. *Comput. Optim. Appl.*, 30(1):45–61, 2005.
- [17] M. Hinze, R. Pinnau, M. Ulbrich, and S. Ulbrich. *Optimization with PDE constraints*, volume 23 of *Mathematical Modelling: Theory and Applications*. Springer, New York, 2009.
- [18] J.-L. Lions. *Optimal control of systems governed by partial differential equations*. Translated from the French by S. K. Mitter. Die Grundlehren der mathematischen Wissenschaften, Band 170. Springer-Verlag, New York, 1971.
- [19] K. Lipnikov, G. Manzini, F. Brezzi, and A. Buffa. The mimetic finite difference method for the 3D magnetostatic field problems on polyhedral meshes. *J. Comput. Phys.*, 230(2):305–328, 2011.
- [20] A. Rösch. Error estimates for linear-quadratic control problems with control constraints. *Optim. Methods Softw.*, 21(1):121–134, 2006.
- [21] F. Tröltzsch. *Optimal control of partial differential equations*, volume 112 of *Graduate Studies in Mathematics*. American Mathematical Society, Providence, RI, 2010. Theory, methods and applications, Translated from the 2005 German original by Jürgen Sprekels.

MOX Technical Reports, last issues

Dipartimento di Matematica “F. Brioschi”,
Politecnico di Milano, Via Bonardi 9 - 20133 Milano (Italy)

- 30/2011** NOBILE, F.; POZZOLI, M.; VERGARA, C.
Time accurate partitioned algorithms for the solution of fluid-structure interaction problems in haemodynamics
- 29/2011** MORIN, P.; NOCHETTO, R.H.; PAULETTI, S.; VERANI, M.
AFEM for Shape Optimization
- 28/2011** PISCHIUTTA, M.; FORMAGGIA, L.; NOBILE, F.
Mathematical modelling for the evolution of aeolian dunes formed by a mixture of sands: entrainment-deposition formulation
- 27/2011** ANTONIETTI, P.F.; BIGONI, N.; VERANI, M.
A Mimetic Discretization of Elliptic Control Problems
- 26/2011** SECCHI, P.; VANTINI, S.; VITELLI, V.
Bagging Voronoi classifiers for clustering spatial functional data
- 25/2011** DE LUCA, M.; AMBROSI, D.; ROBERTSON, A.M.; VENEZIANI, A.; QUARTERONI, A.
Finite element analysis for a multi-mechanism damage model of cerebral arterial tissue
- 24/2011** MANZONI, A.; QUARTERONI, A.; ROZZA, G.
Model reduction techniques for fast blood flow simulation in parametrized geometries
- 23/2011** BECK, J.; NOBILE, F.; TAMELLINI, L.; TEMPONE, R.
On the optimal polynomial approximation of stochastic PDEs by Galerkin and Collocation methods
- 22/2011** AZZIMONTI, L.; IEVA, F.; PAGANONI, A.M.
Nonlinear nonparametric mixed-effects models for unsupervised classification
- 21/2011** AMBROSI, D.; PEZZUTO, S.
Active stress vs. active strain in mechanobiology: constitutive issues